WATER ABSORPTION AND DESORPTION BEHAVIOUR AND THEIR EFFECT ON THE TENSILE PROPERTIES OF FM 73M ADHESIVE FILM

Sugiman[1*], Sulardjaka[2]

[1] *Department of Mechanical Engineering, Faculty of Engineering, University of Mataram, Mataram, Indonesia*
[2] *Department of Mechanical Engineering, Faculty of Engineering, Diponegoro University, Semarang, Indonesia*

ABSTRACT

Structural adhesives have been widely used to join metal to metal, and metal to composite in automotive and aircraft structures. However, the adhesive is susceptible to water absorption from the surrounding environment and this affects the mechanical properties of the adhesive, leading to reduction in the performance of the structure. This paper investigated the water absorption and desorption behaviour of FM 73M structural adhesive film and its effect on the tensile properties. The adhesive was immersed in deionised water at a temperature of 50°C. A gravimetric method was carried out to obtain the water uptake. Dog bone specimens were used to investigate the residual tensile strength of the adhesive. Finite element modelling was performed to model the spatial moisture distribution in the adhesive and the residual tensile strength after having absorbed water. It was found that the water absorption of FM 73M deviated from Fick's second law, however the desorption behaviour followed Fick's second law. The tensile properties of the adhesive (the tensile strength and the elastic modulus) tend to decrease with the increase of water content and they are recovered after desorption at the same temperature as the absorption. The residual tensile strength was predicted using a continuum damage approach combined with environmental degradation. Good agreement has been found between the predicted and the experimental results.

Keywords: Adhesive; Finite element modelling; Tensile properties; Water absorption

1. INTRODUCTION

One of the disadvantages of using adhesive in adhesive joint and polymeric matrix composites is that adhesive absorbs water from the surrounding environment. The absorbed water induces plasticization of the adhesive that eventually reduces the mechanical properties of adhesive and the structures where the adhesive is used.

The behaviour of water diffusion into the adhesive depends on many factors, such as the surrounding water concentration, temperature, microstructure of the adhesive, thickness of the adhesive and exposure time. It has been reported in the literature that water diffusion could either follow the Fickian diffusion or deviate from the Fickian diffusion. Carter and Kibler (1978) studied water diffusion in 5208 epoxy resin and found that the water diffusion deviated from the Fickian diffusion. Furthermore, they used the Langmuir diffusion model to describe what the absorbed water might be in the form of bound and free water. Many forms of non-

*Corresponding author's email: s.sugiman@unram.ac.id Tel. +62-370-636087, Fax. +62-370-636523

Fickian diffusion were proposed such as a dual Fickian diffusion (Loh et al., 2005; Placette et al., 2012), a sequential dual Fickian (Ameli et al., 2011), and an exponential Fickian (Mubashar et al., 2009).

Experimental works reported in the literature showed the degradation of adhesive after being exposed in the moist environment, such as glass transition temperature (Zhou & Lucas, 1999b; Lettieri & Frigione, 2012), the tensile strength, the elastic modulus (Zafar et al., 2012; Han et al., 2014) and the fracture toughness (Butkus et al., 1998; Quino et al., 2014). However, numerical works such as finite element modelling to predict the residual strength of adhesive after being exposed in the moist environment are still rarely reported. This paper presents the water diffusion in a structural adhesive and numerically predicts the spatial water distribution in the adhesive and furthermore, the residual tensile strength of the adhesive after being exposed in water at a temperature of 50°C.

2. DISPARITY LINE UTILIZATION FACTOR

2.1. Bulk Adhesive Manufacturing

To investigate the water uptake behaviour in FM 73M bulk adhesive, a plate of bulk adhesive was made by stacking eight layers of FM 73M film. The film is green with random (mat) polyester carrier. It has a nominal thickness of 0.13 mm with one side smooth and tacky. Strips of adhesive were cut into 150 mm long and 12 mm wide pieces and then stacked one by one on silicon-coated plastic film with a clean glass plate as a base. A light pressure was applied on the adhesive to remove air trapped during stacking. After all the layers of film adhesive had been positioned, the stack was then put in the vacuum oven to release any remaining air. The temperature of the vacuum oven was set at 90°C to allow the adhesive to flow and to help in releasing the air bubbles when the vacuum oven was operating. This vacuuming process took approximately an hour before transferring it to the Carbolite programmable curing oven where the cure temperature can be controlled more precisely.

During curing, a deadweight tester was applied to provide a pressure of 0.11 MPa. The adhesive thickness was maintained at approximately 0.8 mm using steel spacers. The adhesive was cured in the oven as recommended by the manufacturers (Cytec, 1998). The temperature was increased from room temperature (approximately 20°C) to 120°C over a period of 30 minutes and then kept constant at 120°C for 60 minutes. After this, the oven was set to stop and temperature decreased to room temperature at a slow rate, with the specimen left in the oven (with the door shut) overnight. This was to avoid residual thermal stresses in the adhesive. The bulk adhesive obtained was very good quality with no observed voids on the surfaces.

2.2. Bulk Adhesive Absorption and Desorption

For water uptake studies, the bulk adhesive was cut to rectangular plates measuring 12mm×18mm×0.823mm. Three specimens were prepared for these studies. For tensile behaviour studies related to the bulk adhesive, the rectangular plates were cut into dog bone-shaped specimens using a CNC machine. Both types of specimens are shown in Figure 1.
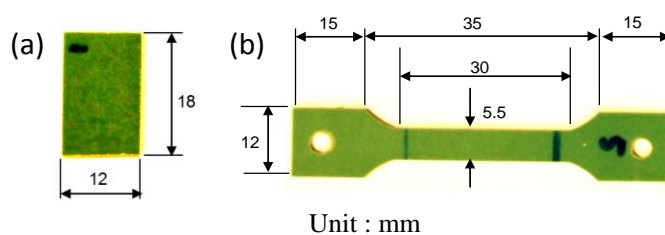

Figure 1 (a) Rectangular bulk for moisture diffusion; (b) Dog bone specimen of FM 73M. Specimen thickness was 0.823 mm

Before ageing, the specimen surfaces were lightly abraded using 2400 grade sand paper to remove any silicon film from the bulk surface. This was to ensure the water would diffuse without any obstacles into the bulk surface. Prior to immersion, the specimens were conditioned in the oven (ambient environment) at a temperature of 50°C to remove the absorbed moisture from the surrounding environment during preparation. The weight of the specimen was measured using a microbalance with 0.1 mg accuracy (Adam Company). After the specimen weight was constant, they were then immersed in deionised water in an oven at a temperature of 50°C. The weight then was measured periodically for a period of time until saturation was achieved. This method is known as the gravimetric method. The specimens were taken out from the deionised water and wiped out using laboratory tissue to remove water on the bulk surface before weighing. The weighing was carried out as fast as possible to avoid the drying process having a significant effect on the absorbed water. The water uptake, M_t was calculated using Equation 1.

$$M_t = \frac{(W_t - W_o)}{W_o} \times 100\% \tag{1}$$

where W_t is the weight at time t, W_o is the initial weight before immersion.

The same procedure as for the rectangular plate was used to measure the moisture absorption of the bulk dog bone specimen. The dog bone specimens were put on a perforated corrugated stainless steel plate in deionised water at a temperature of 50°C. After a period of time, these dog bone specimens were taken out from the deionised water to be statically tested to investigate the water dependent tensile properties.

Desorption of the rectangular plates and the dog bone specimens was done in the oven, at a temperature of 50°C. This procedure was performed immediately after the water diffusion. The same weight measurement as water absorption was carried out during this desorption, until the weight was constant. This was to investigate the behaviour of desorption of bulk adhesive. The results were then compared with the absorption behaviour. The dog bone specimens were statically tested to determine the residual strength after desorption.

From the experimental water uptake, data fits were carried out to investigate the water uptake behaviour. For Fickian diffusion, according to Fick's second law, the water uptake with time into an infinite plate with a thickness of *2l* follows Equations 2 and 3 (Crank, 1975).

$$M_t = M_\infty \left(1 - \frac{8}{\pi^2} \sum_{n=0}^{\infty} \frac{1}{(2n+1)^2} \exp\left[\frac{-(2n+1)^2 \pi^2 D t}{4l^2} \right] \right) \tag{2}$$

$$D = \frac{\pi}{t} \left(\frac{l}{4} \right)^2 \left(\frac{M_t}{M_\infty} \right)^2 \tag{3}$$

where D is the diffusion rate, M_∞ is the water uptake at equilibrium. However, some polymers can have different water uptake behaviours. One of those is called as a sequential Fickian diffusion (SDF), where two simple Fickian (SF) diffusions with different diffusion rate occur sequentially as described in Equations 4 and 5 (Ameli et al., 2011).

$$M_t = \left(1 - \frac{8}{\pi^2}\sum_{n=0}^{\infty}\frac{1}{(2n+1)^2}\exp\left(\frac{-D_1(2n+1)^2\pi^2 t}{4l^2}\right)\right)M_{1\infty} +$$

$$\phi(t-t_d)\left(1 - \frac{8}{\pi^2}\sum\frac{1}{(2n+1)^2}\exp\left(\frac{-D_2(2n+1)^2\pi^2(t-t_d)}{4l^2}\right)\right)M_{2\infty} \qquad (4)$$

$$\phi(t-t_d) = \begin{cases} 0, & t < t_d \\ 1 & t \geq t_d \end{cases} \qquad (5)$$

Parameters D_1 and D_2 are the diffusion rate of the first and the second stage of absorption respectively, $M_{1\infty}$ and $M_{2\infty}$ indicate the water equilibrium at the first and second stage absorption respectively, t_d is the transition time from the first to the second absorption. A $\Phi(t)$ is the Heaviside step function.

2.3. Mechanical Testing

The tensile test of dog bone specimens was carried out using an Instron testing machine with a load cell capacity of 1 kN. The displacement rate was 0.1 mm/min. An extensometer with a gauge length of 10 mm was attached onto the specimen to measure the elongation during testing.

3. RESULTS AND DISCUSSION

3.1. Mechanical Testing

Figure 2 shows the water uptake and desorption with square root time over adhesive thickness of the FM 73M adhesive. It seems that the absorption process has two stages; the first stage ended at the water uptake of approximately 3.6% after 17 days and then it was followed by the second stage with much slower absorption rate than the first stage. A SF model did not agree well with the water uptake data; however it was in good agreement with the SDF model. The water equilibrium for SF was fitted at 4.39%, but indeed the water uptake equilibrium reached 5.6% (not shown in Figure 2). The properties of water absorption are shown in Table 1. The second absorption was related to the formation of microvoids after a long-term exposure due to leaching of the backbone of the polymer chain, chain scissor (Xiao & Shanahan, 1997) leaving unoccupied sites in the polymer. This may be followed by the polymer chemical degradation shown by the changing colour. It is also believed that the second absorption stage is due to the polymer relaxation process where more swelling takes place, resulting in redistribution of voids and free volume (Jiang et al., 2014).

Table 1 Coefficient of water diffusion and water equilibrium for FM 73M

	D_1, mm^2/day	D_2, mm^2/day	$M_{1\infty}$ (wt %)	$M_{2\infty}$ (wt %)	t_d, day (s)
Absorption SF	0.031	-	4.39	-	-
Absorption SDF	0.048	1.8×10^{-4}	3.60	2	17
Desorption SF	0.150	-	3.30	-	-

After absorption, at the water uptake of approximately 4.6% the specimen was desorbed at the same temperature of absorption. In this case, the desorption behaviour obeyed the Fickian diffusion. However, there was a residual amount of water that remained in the polymer,

approximately 1.09%. Zhou and Lucas (1999a) showed the same behaviour when they studied the absorption-desorption of epoxy resin. They suggested that there were two kinds of bound water; Type 1 and Type 2, respectively, which are related to single hydrogen bonding and the van der Waals interaction, and multiples of hydrogen bonding of water molecules with the polymer chain. Type 1 is weaker than Type 2 and easy to desorp, while the strong bound water (Type 2) needs higher energy (temperature) to break the bonding. The later is related to the residual water after desorption.
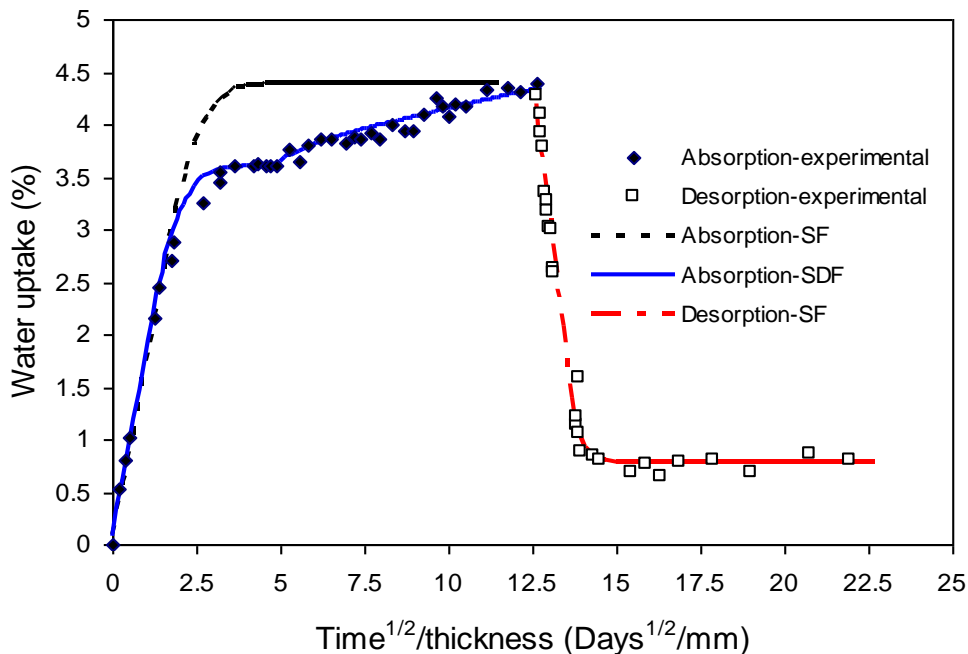

Figure 2 Water absorption and desorption of FM 73M

3.2. Tensile Behaviour

Figure 3a shows the stress-strain responses of FM 73M adhesive with the water content up to 5.5%. It can be seen that with increasing water content, the slope of curves tended to decrease, as well as the ultimate tensile stress. However, the strain at fracture tended to increase, even though there were scattered data. The trend of decreasing elastic modulus and tensile strength is shown in Figure 4. It appears that the decreasing tensile strength was higher than that of the elastic modulus. The water residing between the polymer chain networks increases the chain mobility, leading to increasing flexibility. This plasticises the polymer and reduces its stiffness and tensile strength.
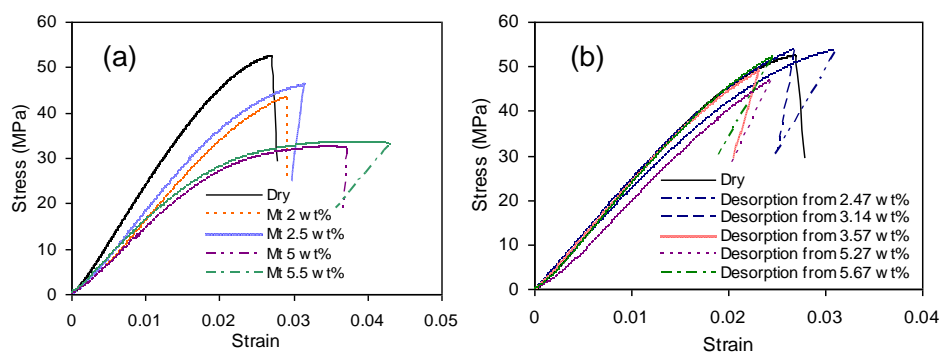

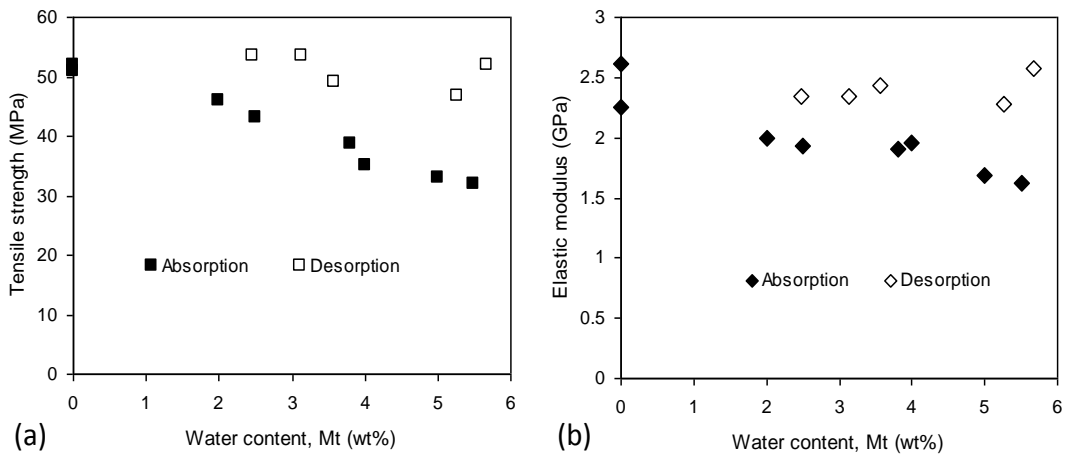Figure 3 Stress-strain curves of FM 73M adhesive after: (a) absorption; (b) desorption

Figure 4 (a) Tensile strength and (b) Elastic modulus of FM 73M at different water content levels

Upon drying, water in the polymer was desorbed and the tensile strength and the elastic modulus were recovered as seen in Figures 3b and 4. Even at high water uptake (greater than 5%) where the permanent degradation might occur, the recovering of the tensile strength and the elastic modulus was still obtained. This might be caused by the multiple hydrogen bondings between the residual water and the polymer chain that were able to increase the elastic modulus (Zhou & Lucas, 1999b), thus compensating for the detrimental effect of the permanent degradation.
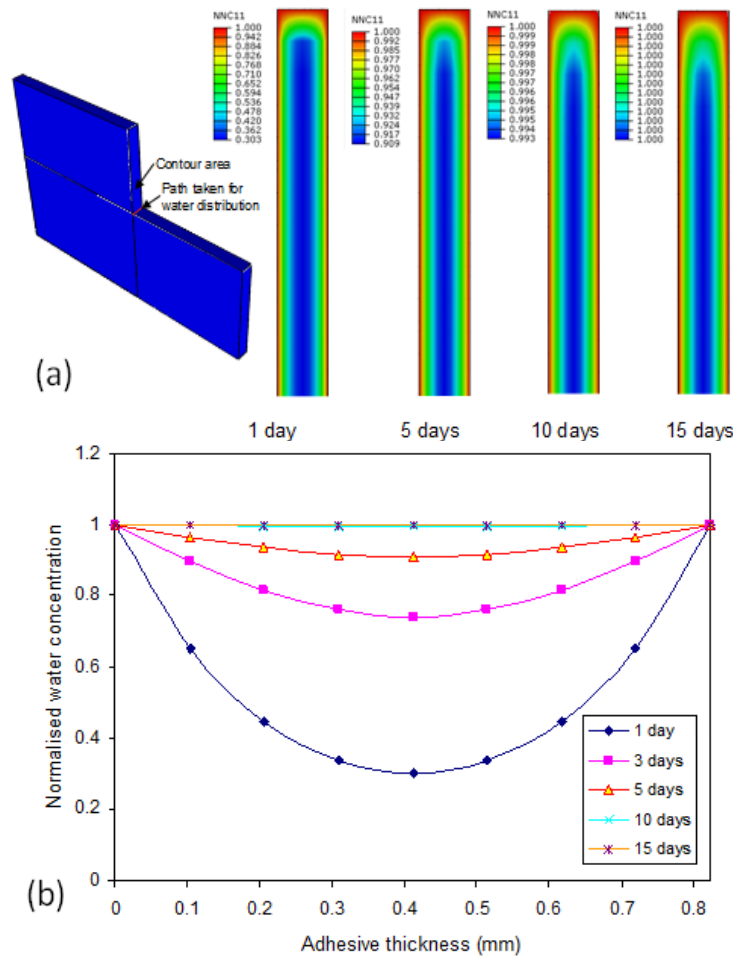

Figure 5 (a) Contour of water; (b) water distribution across the thickness of FM 73M at different immersion time

4.   FINITE ELEMENT MODELLING (FEM)

4.1.   Water Diffusion

To model water diffusion in FEM, a mass diffusion was applied. The mass diffusion in ABAQUS (2009) is an extension of Fick's law according to Equation 6.

$$J = -sD\left[\frac{\partial \varphi}{\partial x} + \kappa_s \frac{\delta}{\delta x}\left(\ln(\theta - \theta^Z)\right) + \kappa_p \frac{\delta p}{\delta x}\right] \tag{6}$$

where J is the flux of concentration, D is the diffusivity, $\varphi = c/s$ is the normalised concentration, c is the concentration of the diffusant, and s is the solubility of the diffusant in the base material, κ_s is the Sorret effect factor, κ_p is the pressure stress factor, θ is the temperature, θ^Z is the absolute zero temperature, p is the pressure and x is the position. By setting s as unity, the diffusion is driven by the concentration gradient only, so that Equation 6 becomes as shown in Equation 7;

$$J = -D\frac{\partial c}{\partial x} \tag{7}$$

Because the specimen was immersed in water, therefore water diffused from four sides of the specimen. A three-dimensional (3D) model was carried out with boundary conditions at four sides that were the normalised concentration of water uptake (NNC) at a fully saturated condition. The Fickian diffusion model was chosen, as it was more convenient and furthermore, most polymers obey the Fickian diffusion, particularly at thick and long path diffusion. The contour plots of normalised absorbed water are as seen in Figure 5a. The water distribution along the adhesive thickness with the path taken at the centre of the specimen (see Figure 5a) is shown in Figure 5b. It is seen that at 5 days, the normalised water uptake has reached above 0.9 and at 15 days the equilibrium water uptake has been reached. Although the diffusion process was from four sides (3D diffusion), the water distribution was taken at the middle of the specimen, so the other effects of water diffusion from the thickness direction were negligible.
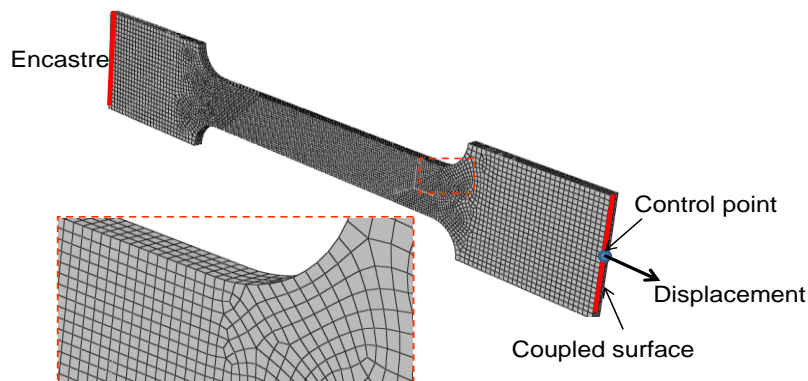

Figure 6 Meshing of a dog bone specimen for finite element modelling

4.2.   Prediction of the Residual Tensile Strength

To predict the residual tensile strength of bulk adhesive, a finite element modelling was carried out utilising a Continuum Damage Model (CDM). This approach is able to model both damage initiation and damage evolution. The framework of this approach can be found elsewhere in the ABAQUS documentation (ABAQUS, 2009). A bulk adhesive was modelled using 3D elements. Boundary conditions and meshing of the bulk adhesive are as shown in Figure 6. The model was clamped (encastre), at one end of, while at the other end, a displacement was

applied at the control point of a kinematic coupling. In the CDM, the damage initiation point was set at the end of plastic strain of the plastic stress-strain curve of bulk adhesive, which was 0.0054. The damage evolution was based on displacement, where the displacement at failure was set as 0.095 mm. The water dependent mechanical properties of bulk adhesive were obtained by defining the normalised concentration as a field variable for the subsequent mechanical analysis. This enables simulating the different mechanical properties with water content, in case the bulk adhesive has not been saturated with water.
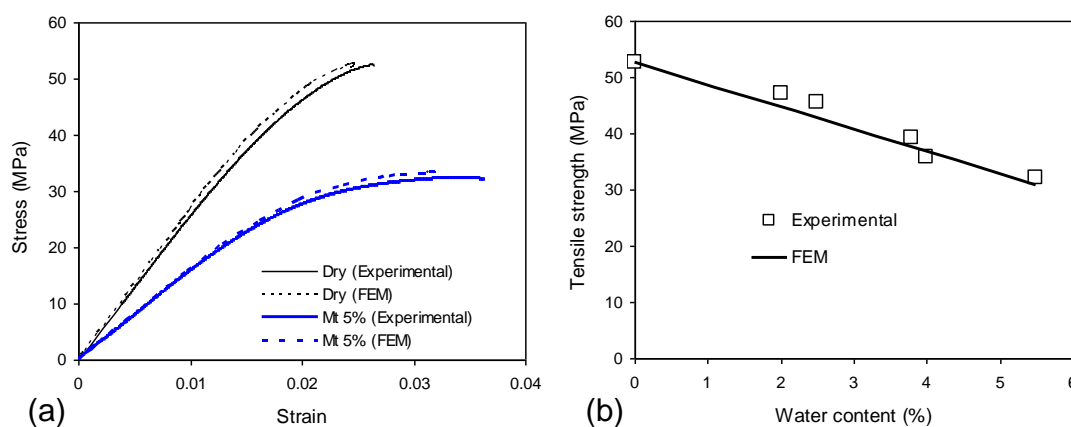

Figure 7 (a) The predicted and experimental stress-strain responses; (b) the predicted and experimental tensile strength of FM 73 at different levels of water content

It can be seen in Figure 7a that the stress-strain responses between the predicted and the experimental results were in good agreement, both at dry and at water content of 5%. The initial predicted and experimental stress-strain curves (at the linier part) were mostly in excellent agreement as the stresses were relatively small and experimentally, the effects of overall machine compliances were negligible. But with increasing the stress, the effects were likely to be more obvious especially on the measured strain; hence the measured strain tended to be higher than the predicted strain. For the dry specimens, where the mechanical properties throughout the specimen were considered homogeneous, the predicted tensile strength was in very good agreement with the experimental result. However for the aged specimens (i.e. at water content of 5%), the predicted tensile strength was slightly higher than the experimental, even the predicted strain at break was much higher. It might be caused by inaccuracy in simulating the spatial water distribution in the adhesive and so the water dependent mechanical properties, such as dependencies of the tensile properties (the tensile strength and the elastic modulus) on water content were assumed to be linear. In practice, the dependencies might not be linear. As for the results, they affected the accuracy in predicting both the tensile strength and the strain. Nevertheless, as seen in Figure 7b, the predicted tensile strength at the different water content levels was also in agreement with the experimental data. The success of this prediction may be extended in predicting the water uptake in composite materials and the residual strength in adhesively bonded joint after being aged in prolonged time.

5. CONCLUSION

The experimental work has been undertaken to investigate the absorption and desorption of water into the FM 73M adhesive and its effect on the tensile properties when immersed in deionised water at a temperature of 50°C. The water absorption behaviour of FM 73M deviates from Fickian diffusion, but desorption does follow Fickian diffusion. Residual water, approximately 1.09%, remains after desorption that is possibly in the form of bound water. The

absorbed water decreases the tensile strength and the elastic modulus of adhesive, due to the plasticisation effect and these are recovered after desorption. Finite element modelling, utilising the continuum damage model, successfully predicts the residual tensile strength of bulk adhesive in the different water content levels.

6.   REFERENCES

ABAQUS, 2009. *User manual*, version 6.9.1, Habbit, Karlsson & Sorensen, Inc., USA

Ameli, A., Datla, N.V., Papini, M., Spelt, J.K., 2011. Hygrothermal Properties of Highly Toughened Epoxy Adhesives. *Journal of Adhesion*, Volume 86, pp. 698–725

Butkus, L.M., Mathern, P.D., Johnson, W.S., 1998. Tensile Properties and Plane Stress Fracture Toughness of Thin Film Aerospace Adhesives. *Journal of Adhesion*, Volume 66, pp. 251–273

Carter, H.G., Kibler, K.G., 1978. Langmuir Type Model for Anomalous Moisture Diffusion in Composite Resins. *Journal of Composite Materials*, Volume 12, pp. 118–131

Crank, J., 1975. *The Mathematics of Diffusion*, 2nd edition. Oxford University Press, London

Cytec Engineered Materials, 1998. FM$^{®}$ 73 *Toughened Epoxy Film*, Technical Service, 1300 Revolution Street. Havre de Grace, Maryland

Han, X., Crocombe, A.D., Anwar, S.N.R., Hu, P., 2014. The Strength Prediction of Adhesive Single Lap Joints Exposed to Long Term Loading in a Hostile Environment. *International Journal of Adhesion & Adhesives*, Volume 55, pp. 1–11

Jiang, X., Kolstein, H., Bijlaard, F., Qiang, X., 2014. Effects of Hygrothermal Aging on Glass-fibre Reinforced Polymer Laminates and Adhesive of FRP Composite Bridge: Moisture Diffusion Characteristics. *Composites: Part A,* Volume 57, pp. 49–58

Lettieri, M., Frigione, M., 2012. Effects of Humid Environment on Thermal and Mechanical Properties of a Cold-curing Structural Epoxy Adhesive. *Construction and Building Materials*, Volume 30, pp. 753–760

Loh, W.K., Crocombe, A.D., Wahab, M.M.A., Ashcroft, I.A., 2005. Modelling Anomalous Moisture Uptake, Swelling and Thermal Characteristics of a Rubber Toughened Epoxy Adhesive. *International Journal of Adhesion and Adhesives*, Volume 25, pp. 1–12

Mubashar, A., Aschroft, I.A., Critchlow, G.W., Crocombe, A.D., 2009. Modelling Cyclic Moisture Uptake in an Epoxy Adhesive. *The Journal of Adhesion*, Volume 85, pp. 711–735

Placette, M.D., Fan, X., Zhao, J.H., Edwards, D., 2012. Dual Stage Modeling of Moisture Absorption and Desorption in Epoxy Mold Compounds. *Microelectronics Reliability*, Volume 52, pp. 1401–1408

Quino, G., Yagoubi, J., Lubineau, G., 2014. Characterizing the Toughness of an Epoxy Resin after Wet Aging using Compact Tension Specimens with Non-uniform Moisture Content. *Polymer Degradation and Stability*, Volume 109, pp. 319–326

Xiao, G.Z., Shanahan, M.E.R., 1997. Water Absorption and Desorption in an Epoxy Resin with Degradation. *Journal of Polymer Science: Part B: Polymer Physics*, Volume 35, pp. 2659–2670

Zafar, A., Bertocco, F., Schjødt-Thomsen, J., Rauhe, J.C., 2012. Investigation of the Long Term Effects of Moisture on Carbon Fibre and Epoxy Matrix Composites. *Composites Science and Technology*, Volume 72, pp. 656–666

Zhou, J., Lucas J.P., 1999a, Hygrothermal Effects of Epoxy Resin. Part I: the Nature of Water in Epoxy. *Polymer*, Volume 40, pp. 5505–5512

Zhou, J., Lucas, J.P., 1999b. Hygrothermal Effects of Epoxy Resin. Part II: Variations of Glass Transition Temperature. *Polymer*, Volume 40, pp. 5513–5522